

CHEMISTRY

A European Journal

A Journal of



Accepted Article

Title: A new lacunary polyoxovanadate precursor and TM-sandwiched derivatives for catalytic oxidation of sulfides

Authors: Jing Yang Niu, Rong Wan, Peipei He, Zhen Liu, Xinyi Ma, Pengtao Ma, Vikram Singh, Chao Zhang, Jingyang Niu, and Jingping Wang

This manuscript has been accepted after peer review and appears as an Accepted Article online prior to editing, proofing, and formal publication of the final Version of Record (VoR). This work is currently citable by using the Digital Object Identifier (DOI) given below. The VoR will be published online in Early View as soon as possible and may be different to this Accepted Article as a result of editing. Readers should obtain the VoR from the journal website shown below when it is published to ensure accuracy of information. The authors are responsible for the content of this Accepted Article.

To be cited as: *Chem. Eur. J.* 10.1002/chem.201905741

Link to VoR: <http://dx.doi.org/10.1002/chem.201905741>

Supported by
ACES

WILEY-VCH

FULL PAPER

A new lacunary polyoxovanadate precursor and TM-sandwiched derivatives for catalytic oxidation of sulfides

Rong Wan, Peipei He, Zhen Liu, Xinyi Ma, Pengtao Ma, Vikram Singh, Chao Zhang, Jingyang Niu* and Jingping Wang*^[a]

[a] R. Wan, P. He, Z. Liu, X. Ma, P. Ma, V. Singh, C. Zhang, Prof. J. Niu*, Prof. J. Wang*.
Henan Key Laboratory of Polyoxometalate Chemistry
College of Chemistry and Chemical Engineering, Henan University
Kaifeng, Henan, 475004, (P. R. China), Fax: (+86)-371-23886876
E-mail: jyniu@henu.edu.cn, jpwang@henu.edu.cn

Abstract: A SeO₃-centered lacunary Keggin-type heteropolyoxovanadate (hetero-POV) K₆H₂[SeV₁₀O₂₈(SeO₃)₃]·14H₂O (**1**) was isolated by one-pot reaction of KVO₃ and SeO₂ under acidic condition. X-ray studies revealed that it comprised a single {VO₅}-capped trivacant B-α-type Keggin ion [SeV₉O₃₃(VO)]¹⁴⁻ with its lacunary sites decorated by three {SeO₃} pyramids. Interestingly, this new basic hetero-POV building block was further used as precursor to assembly with different transition metal (TM) ions, yielding a series of TM-sandwiched POVs K₆H₈[(SeV₁₀O₂₈(SeO₃)₃)₂(M(H₂O)₄)]·24H₂O (M²⁺ = Mn²⁺ (**2**), Co²⁺ (**3**), Zn²⁺ (**4**)). All four compounds were characterised by single-crystal X-ray structure analysis, IR, XPS, EPR, and ⁵¹V NMR spectroscopy. Importantly, three TM-sandwiched derivatives exhibited effectively catalytic activity for the heterogeneous oxidative desulfurization of sulfides at room temperature.

Introduction

With compelling features especially chemical and functional tunability, polyoxometalates (POMs) render a fascinating structural and compositional diversity, and a multitude of significant applications in academic and applied sciences, for example catalysis, photo-/electrochemistry, and materials chemistry.¹ Traditionally, POMs are metal-oxide-based clusters, therefore, based on their component transition metals, polyoxotungstates (POTs), polyoxomolybdates (POMos), and polyoxovanadates (POVs) are known as the most important and vibrant subsets.² However, being different from molybdenum and tungsten which usually formed octahedral {M^{VI}O₆} units in their cluster frameworks, vanadium in POVs is apt to display mixed-valent states with flexible coordination geometries (normally tetrahedral {V^{VO}O₄}, square-pyramidal {V^{VO}O₅} and {V^{VO}O₅}, octahedral {V^{VO}O₆} and {V^{VO}O₆}).³ Due to such versatility in redox behaviors, POVs can be opted as a promising candidate in catalysis, magnetism and electrode materials, thus always being preferred among researchers working in this area.⁴

Generally, the reported structures of POVs can be roughly divided into two families, iso-POVs and hetero-POVs. So far, the chemistry of hetero-POVs has achieved great success as the introduction of heteroatoms tremendously broaden the scope of hetero-POVs synthetic, structural and applied chemistry.^{3c,5-11} In particular, the representative works were contributed by research groups of Müller, Wang, Hu, Yang and so on, and the most renowned findings in this subclass embraced but not limited to {MV_{13/14}} (M = Mn, Ni),^{4d,6} {XV₁₄} (X = Al, P, As, Ge)⁷ and

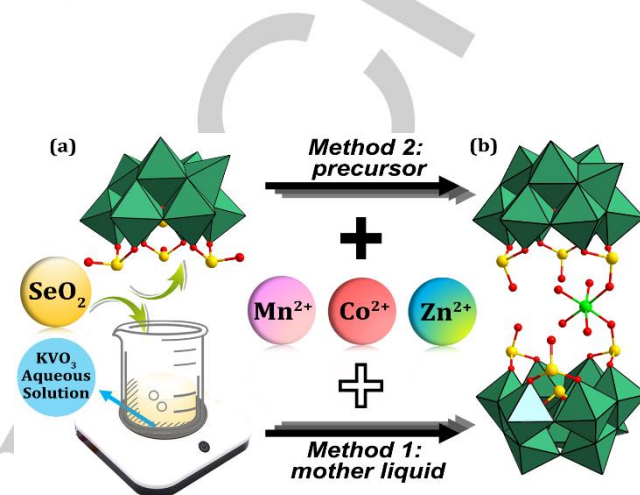


Figure 1. The two synthetic methods of compounds 1–4. Combined polyhedral/ball-and-stick representations of (a) a new type of hetero-POV [SeV₁₀O₂₈(SeO₃)₃]⁸⁻ (**1a**); (b) polyanions [(SeV₁₀O₂₈(SeO₃)₃)₂(M(H₂O)₄)]¹⁴⁻ (M = Mn²⁺ (**2a**), Co²⁺ (**3a**), Zn²⁺ (**4a**)). Colour code: polyhedral V^{VO}O₅ and V^{VO}O₆, green; Se, yellow ball; O, red ball, TMs, green ball.

{X_{2n}V_{18-n}} (X = Si, Ge, As, Sb, n = 2–4)⁸⁻¹¹ (Scheme S1). Moreover, some of these backbones could be further modified by organic moieties and transition metal (TM) complexes, leading to a continuous expansion of this subfamily.¹² However, compared with extensive works on hetero-POVs functionalized by TMs and semimetals from group 14 and 15 elements (mostly Si, Ge, As, and Sb), the reports regarding POVs encapsulating elements located at group 16 on the periodic table, especially Se element, has hardly any weight. To our knowledge, only two Se-substituted POVs [SeV₃O₁₁]³⁻ and [Se₂V₂O₁₀]²⁻ were isolated by Nakano and co-workers in 2001,¹³ which were constructed from tetrahedral VO₄ and trigonal pyramidal SeO₃ motifs to form ring-like structures by sharing vertices (Figure S1). Such an apparent blank in the investigation of Se-containing POVs have allowed us to gain deep insights to study the mystery of assembling new type of hetero-POVs together with their applications.

In this work, a new type of hetero-POV precursor K₆H₂[SeV₁₀O₂₈(SeO₃)₃]·14H₂O (**1**) was isolated by reacting SeO₂ with KVO₃ (Figure 1a), featuring one {VO₅}-capped trivacant Keggin unit [B-α-SeV₉O₃₃] with its vacant sites being occupied by three {SeO₃} groups. Interestingly, by employing different TM²⁺ ions to assemble with this isolated vanadoselenite cluster or mixture of KVO₃ and SeO₂, a family of vanadoselenite-based TM-derivatives K₆H₈[(SeV₁₀O₂₈(SeO₃)₃)₂(M(H₂O)₄)]·24H₂O (M²⁺ = Mn²⁺ (**2**), Co²⁺ (**3**), Zn²⁺ (**4**)) were prepared (Figure 1b), and each of them existed a closely related structure of *in-situ* formed vanadoselenite building block of {SeV₁₀O₂₈(SeO₃)₃} (aliased as

FULL PAPER

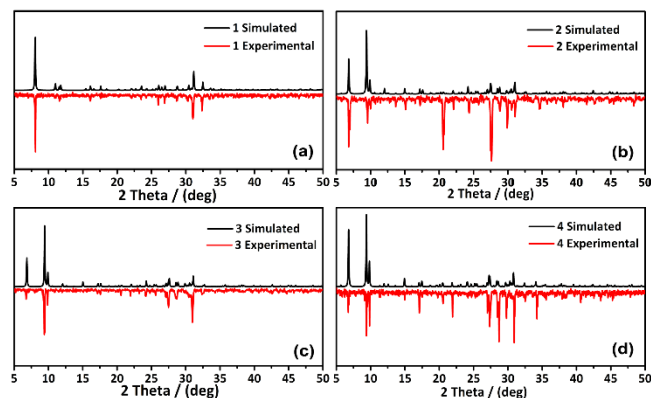


Figure 2. The experimental and simulated PXRD patterns for the bulk products of (a–d) **1–4**.

{Se₄V₁₀}), which is also observed for the first time in POM chemistry. These four vanadoselenites were also structurally characterized by X-ray single crystal diffraction (Table S1), XRPD, IR spectra (Figure S2), XPS, EPR and TGA analyses (Figure S3), and then employed as heterogeneous catalysts toward the catalytic oxidation of sulfides under mild conditions.

Results and Discussion

Crystal Structure

The experimental powder XRD (PXRD) patterns of the targeted samples of **1–4** are in good agreement with their simulated PXRD patterns derived from single-crystal X-ray diffraction, respectively, revealing that the samples used for further characterizations and catalytic tests are pure (Figure 2). It should be noted that precursor **1** and its TM-sandwiched derivatives **2–4** exhibit obviously different characteristic peaks in the same range of 2θ angles because of space group difference, while powder XRD patterns of samples **2–4** are nearly the same because they are isostructural with negligible lattice parameter difference.

Single-crystal X-ray diffraction analysis shows that **1** crystallized in the monoclinic space group *Cm*, and comprised a novel polyanion [SeV₁₀O₂₈(SeO₃)₃]⁸⁻ (**1a**). In this new-found vanadoselenite (Figure 1a and Figure 3a), three {V₃O₁₃} triads combined together tightly in a corner-shared fashion with a {SeO₃} group as a center, leading to a trivalent *B-α*-Keggin polyanion [SeV₉O₃₃]¹⁷⁻ just like those trivalent Keggin-type POT cousins [B-*α*-XW₉O₃₃]⁹⁻ (X = As, Si, P, Ge, Se),¹⁴ and the capping penta-coordinate {VO₅} unit was just grafted to four μ₂-oxo bridges at the window of two adjacent {V₃O₁₃} triads. Note that the V6 atom is found to be statistically half-occupancy disordered for two mirror-symmetric positions, then, the structure of **1a** was presented in brief (Figure S4). In this way, such a unique vanadoselenite cluster could be described as a single-capped trivalent *B-α*-type Keggin ion [SeV₉O₃₃(VO)]¹⁴⁻, of which the lacunary sites are occupied by three {SeO₃} trigonal pyramids. Here, it is worth noting that {SeO₃} pyramidal units were used as not only templates for formation of new building block but also protective agents that effectively stabilizing the highly negative-charged [SeV₉O₃₃(VO)]¹⁴⁻ unit. Indeed, the template effect of lone pair-containing ions like SeO₃²⁻ in POMs chemistry is well-known and

a number of examples have been reported in the recent investigations,^{15,16} classical hetero-POTs containing selenium(IV) included TM-sandwiched structures [Cu₃(H₂O)₃(*α*-SeW₉O₃₃)₂]¹⁰⁻, [M₄(H₂O)₃(*α*-SeW₉O₃₃)₂]⁽¹⁶⁻⁴ⁿ⁾⁻ (M = Cr³⁺, Mn²⁺, Fe³⁺, Co²⁺, Ni²⁺, Zn²⁺, Cd²⁺) and [Se₂W₂₁O₆₉(H₂O)]⁴⁻ based on trivalent Keggin {SeW₉} unit,^{16a,16b} dimeric [Mn₄Se₆W₂₄O₉₄Cl(H₂O)₆]¹³⁻, trimeric (Se₂W₁₂O₄₆(WO(H₂O))₃)²⁴⁻ and tetrameric [Se₈W₄₈O₁₇₆]³²⁻ assemblies constructed from hexavacant Dawson {Se₂W₁₂} unit,^{16c,16d} while researches on selenium(IV)-containing hetero-POMs are dominated by a series of carboxylate ligands functionalized POMs [SeMo₆O₂₁L₃]⁴⁻ (L = glycine, β-alanine, acetic acid), [(SeMo₆O₂₁)₂L₃]¹⁰⁻ (L = oxalic acid, succinic acid, adipic acid, suberic acid, 1,3,5-tris(carboxymethoxy)benzene) and [(SeMo₆O₂₁)₆L₁₀]³²⁻ (L = pyridine-2,6-dicarboxylic acid).^{16e-g} These units [SeW₉O₃₃]⁸⁻, [Se₂W₁₂O₄₆]¹²⁻ or [SeMo₆O₂₁]⁴⁻ as-mentioned above are always generated *in-situ*, and no simple salts of them have been isolated and structurally characterized to date. To our knowledge, few hetero-POV precursors have been isolated and used to further construct their derivatives. Therefore, the unique {Se₄V₁₀} cluster provides a new type of topology to the limited family of hetero-POV clusters, which could apply as a useful precursor in further synthetic study. A strong confirmation is that the direct assembly of this isolated cluster {Se₄V₁₀} with different TM²⁺ ions in the ratio of 2: 1 resulted in a family of TM-sandwiched derivatives K₆H₈[(SeV₁₀O₂₈(SeO₃)₃)₂(M(H₂O)₄)]·24H₂O (M²⁺ = Mn²⁺ (**2**), Co²⁺ (**3**) Zn²⁺ (**4**)).

Structural analysis elucidated that **2–4** are crystallized in the hexagonal space group *P3₂21*, occupying the isostructural assemblies, in which there are two symmetrically-related subunits [SeV₁₀O₂₈(SeO₃)₃]⁸⁻, directly held together by one TM²⁺ ion (TM = Mn, Co, Zn), generating the sandwiched architectures (Figure 1b and Figure 3b). As shown in Figure 3, *in-suit* formed polyanion [SeV₁₀O₂₈(SeO₃)₃]⁸⁻ can also be regarded as one {VO₅}-capped trivalent Keggin ion [B-*α*-SeV₉O₃₃]¹⁷⁻ decorated by three trigonal-pyramidal {SeO₃} moieties with their lone pairs directed at outside but rather at the inside as polyanion **1a**. The six-coordinated TM²⁺ ion resides in a distorted octahedron, in which the mid-plane is occupied by three water molecules and one oxygen of the {SeO₃} moiety, whereas the axial sites are defined by a water ligand and one oxygen from the other {SeO₃} moiety in the second subunit (Mn–O: 2.120(3)–2.180(3) Å; Co–O: 2.100(2)–2.120(19) Å; Zn–O: 2.084(14)–2.133(13) Å) (Figure S5, Table S2). Thus, only a patch of area was left in the sandwiched belt, which cannot afford localization of any more sandwiched {M(H₂O)₄O₂}²⁺ fragments, even if increasing the dosage of TM salts in the synthesis system. The observations mentioned above can led to following conclusions with respect to the formation of **1–4** in aqueous acidic medium: (a) precursor **1** and its derivatives **2–4** all comprise the

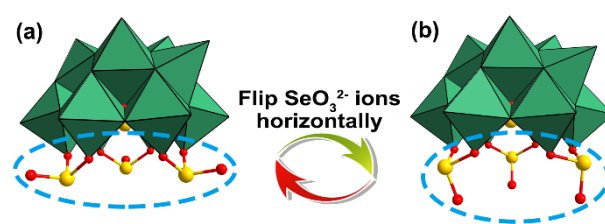


Figure 3. Combined polyhedral/ball-and-stick representation of polyanions (a) [SeV₁₀O₂₈(SeO₃)₃]⁸⁻ (**1a**), and (b) *in-suit* formed subunit [SeV₁₀O₂₈(SeO₃)₃]⁸⁻ in polyanions **2a–4a**.

FULL PAPER

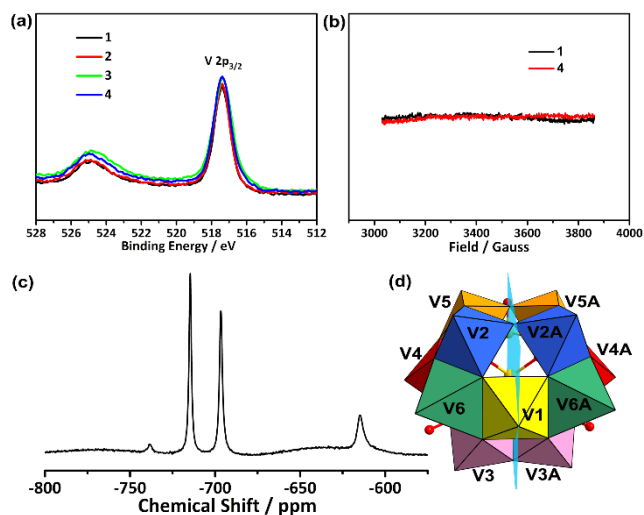


Figure 4. XPS spectra of V 2p (a) in 1–4; (b) Solid state EPR spectra of 1 and 4 at room temperature; (c) Solution ^{51}V NMR spectrum of 1 ($\text{H}_2\text{O}/\text{D}_2\text{O}$, 293 K); (d) The mirror symmetry (light blue plane) in 1 resulted in six kinds of unique vanadium atoms.

metastable hetero-POV cluster $[\text{B-a-SeV}_9\text{O}_{33}]^{17-}$ with high negative charge, which can be trapped and stabilized by electrophilic protecting groups like $\{\text{SeO}_3\}$ and $\{\text{VO}_5\}$ groups; (b) a limited number (actually only one) of the $\{\text{M}(\text{H}_2\text{O})_4\text{O}_2\}^{2+}$ fragment could be bound to the sandwiched belt of two trivalent Keggin-type vanadoselenites because of steric hindrance; (c) coordination with TM^{2+} ions turns the lone pairs of $\{\text{SeO}_3\}$ moieties from inside to outside in 2–4, that is, the coordination position flips horizontally.

XPS, EPR and ^{51}V NMR

Vanadium is a highly specific element, which is known for wide range of oxidation states varying from +2 to +5, then X-Ray photoelectron spectroscopy (XPS) was performed to characterize their oxidation states. As shown in Figure 4a, the V 2p $_{3/2}$ signals of 1–4 in signals all centered at a binding energy of approximately 517.3 eV, which are ascribed to V^{V} centers.¹⁷ The results of the EPR investigations shown in Figure 4b also confirmed this expectation, because EPR spectra of 1 and 4 were all silent that consistent with d^0 electronic configuration in $\text{V}(\text{V})$ centers. In contrast, the obvious paramagnetic signals of can be detected in derivatives 2 and 3 owing to the presence of unpaired electrons in Mn^{2+} (d^5) and Co^{2+} (d^7) ions, respectively (Figure S6).¹⁸

During the course of this study, we also investigated the solution properties of diamagnetic 1 and 4 by ^{51}V NMR measurements in $\text{D}_2\text{O}/\text{H}_2\text{O}$ at room temperature. The ^{51}V NMR spectrum of 1 exhibited only four obvious peaks ($\delta = -614.7$, -696.5 , -714.6 , and -738.4 ppm) rather than the expected six peaks (Figure 4c and 4d). It is assumed that a broadening resonance arising from the background between -680 and -600 ppm may correspond to the missing ^{51}V NMR resonances, while we could not assign them confidently. Possible reasons for this phenomenon are ^{51}V as a quadrupolar nucleus with significant quadruple coupling constants, being highly sensitive to the symmetry of the VO_x polyhedron, which made absolute chemical shift predictions more difficult.¹⁹ As for the diamagnetic 4, ^{51}V NMR

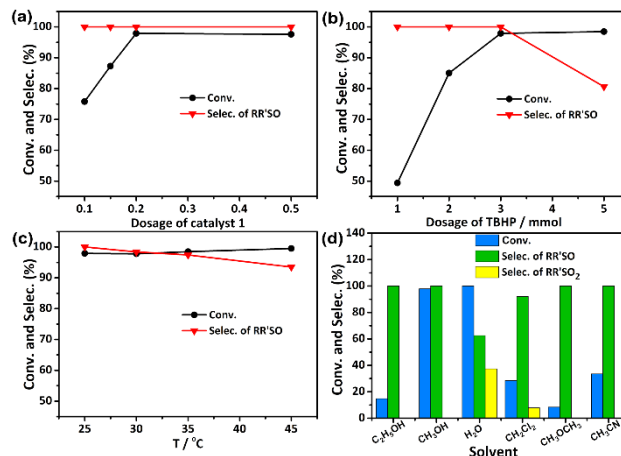


Figure 5. The relationships between the conversion/selectivity of oxidative products (RR'SO: methyl phenyl sulfoxide; RR'SO₂: methyl phenyl sulfone) and (a) the dosage of catalyst 4, (b) the dosage of TBHP (oxidant agent), (c) reaction temperature, and (d) solvent.

spectrum also indicated the presence of four main peaks at -615.3 , -698.1 , -716.6 , and -734.4 ppm as well as a very broad signal between -680 and -600 ppm (Figure S7). By contrast, though 1 and 4 showed very similar ^{51}V NMR spectra owing to their structurally-related building unit $\{\text{Se}_4\text{V}_{10}\}$, three ^{51}V NMR resonances in 4 was found slightly upfield while one signal showed a little downfield relative to those normal positions in 1, which may stem from that the introduction of Zn atom interfered with the anisotropy of electron density of vanadium atoms, thus resulting in the slight differences of the observed ^{51}V NMR chemical shifts.²⁰

Catalysis

Considering the environmental protection and economic benefits into account, it is crucial to remove sulfur species from sulfur-containing compounds to transform them into valuable products, for that oxidative desulfurization has been investigated as a promising strategy.²¹ As was authenticated by previous studies, POVs were found to be fruitful in the oxidation catalysis of sulfides owing to their fast reversible multielectron transformation activity.^{6c,22} Then, the oxidation of methyl phenyl sulfide (a commonly used model substrate) was chosen as a benchmark system to assess the catalytic activity of compounds 1–4. Initially, compound 4 was employed as a catalyst for preliminary investigations on analyzing optimal reaction conditions, because it is the most abundant of yield. After applying a series of controllable tests, the optimized reaction condition for selective oxidation of methyl phenyl sulfide to corresponding sulfoxide was proved to be entry 4, of which 2 μmol catalyst loading with 3 mmol *tert*-butyl hydrogen peroxide (TBHP) in methanol for one hour at room temperature, allowed for achieving excellent conversion (97.9%) and selectivity (100%) (Figure 5, Table S3). Kinetic studies (Figure S8) stated that the catalytic reaction follow first-order dependences over 25–45 °C with apparent activation energy E_a of about 0.226 KJ mol^{-1} .

Under afore-mentioned condition, a hot filtration experiment was performed, of which sulfoxide product was no further increased once catalyst 4 was removed from the reaction system

FULL PAPER

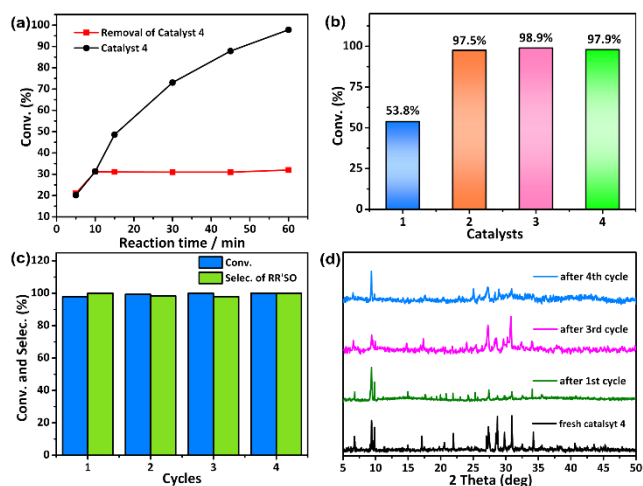


Figure 6. (a) Hot filtration experiment for proving the nature of heterogeneous catalyst **4**; (b) Catalytic oxidative reaction of methyl phenyl sulfide by different catalysts including compounds **1–4**; (c) Recycling of catalyst **4** for the catalytic reaction; (d) XPRD patterns of catalyst **4** before and after the catalytic reaction. Reaction conditions: methyl phenyl sulfide (1 mmol), catalyst (2 μ mol), CH_3OH (2.5 mL), TBHP (3 mmol), 25 $^\circ\text{C}$, 60 min.

after 10 min (Figure 6a), suggesting that this oxidation process is heterogeneous. And not surprisingly, **2** and **3** as heterogeneous catalysts also can catalyze the oxidation of methyl phenyl sulfide to the corresponding sulfoxide with commendable conversion of 96.3%–98.8% and selectivity of 100% (Figure S9, Table S4). From Figure 6b, the new-found hetero-POV **1** itself show moderate catalytic activity (53.8%), while TM-derivatives **2–4** exhibited significantly enhanced catalytic properties. It seemed that both POV components and TM^{2+} ions (Mn^{2+} , Co^{2+} , Zn^{2+}) contributed to promoting catalytic reaction system efficiently. For the purpose of probing the role of each active center of **4** in the oxidation of sulfide, the activity of $\text{Zn}(\text{OAc})_2 \cdot 2\text{H}_2\text{O}$, SeO_2 and KVO_3 were also studied. As shown in Table S4, the conversion of sulfide is quite low or moderate when using $\text{Zn}(\text{OAc})_2 \cdot 2\text{H}_2\text{O}$ (7.7%), SeO_2 (14.0%) or KVO_3 (58.6%) as catalysts. However, the mixture of $\text{Zn}(\text{OAc})_2/\text{KVO}_3$ as homogeneous catalyst led to obviously improved conversion of methyl phenyl sulfide (76.1%). Similarly, the conversion was also increased (73.8%) when the catalyst was a simple mechanical mixture of **1** and $\text{Zn}(\text{OAc})_2 \cdot 2\text{H}_2\text{O}$ with a molar ratio of 2 : 1. In the light of the above results, it can be surmised that the “fusion” of TM^{2+} ions and POV $\{\text{Se}_4\text{V}_{10}\}$ units in **2–4** might synergistically impact the catalytic sulfoxidation process, which led to the improvement of the resultant catalytic performance.^{4c,22a,22b}

Except excellent performance, stability and generality are another two vital criteria in the viability of a catalyst. Then, compound **4** was also selected to examine the long-term stability in a heterogeneous system. After each reaction completion, the catalyst can be easily separated from the reaction mixture by filtration and further reused directly in the subsequent sulfoxidation reactions (Figure S10). After four consecutive uses of catalyst **4**, the conversion of methyl phenyl sulfide showed negligible change in activity (Figure 6c). Moreover, IR spectra (Figure S11), XPRD patterns (Figure 6d) and XPS spectra (Figure S12) of catalyst **4** after four cycles were still identical with those of the as-synthesized catalyst, indicating that it maintains its structural integrity after catalytic experiments.

Finally, the catalytic generality of **4** for sulfoxidation reaction was examined by using various alkyl and aryl sulfides, especially some derivatives of methyl phenyl sulfide with different electronic and steric characters under optimized conditions, the results of which are given in Table S5. It is worthy to mention that the catalytic activity for dialkyl sulphides (entries 1 and 2) showed high efficiency for a shortened reaction time of 25 minutes. On basis of comparison with methyl phenyl sulphide, ethyl phenyl sulfide (entry 3) afforded similar efficiencies of conversion but lower selectivity under the similar conditions, while a higher reaction temperature was required for diphenyl thioether (entry 4) due to its large steric hindrance. Regarding substituted derivatives of methyl phenyl sulphide (entries 5–12), only a very small difference in catalytic activity was observed when para-position and meta-position of the aryl ring were substituted by electron donor or acceptor groups, however, if a substituent was introduced to the ortho-position of aryl ring, owing to larger steric hindrance, it could only acquire a significant decreased catalytic activity in this catalytic system. Thus, the steric hindrance effect of aryl sulphides is suspected to be the main factor affecting the yield of sulfoxide products.^{22c-e}

Conclusion

In summary, a new type of POV cluster $\text{K}_6\text{H}_2[\text{SeV}_{10}\text{O}_{28}(\text{SeO}_3)_3] \cdot 14\text{H}_2\text{O}$ (**1**) featuring a $\{\text{VO}_5\}$ -capped trivacant Keggin-type $\{\text{B-}\alpha\text{-SeV}_9\}$ cluster was proposed in this work, and with the introduction of TM^{2+} ions on this base, a series of sandwiched hetero-POVs $[(\text{SeV}_{10}\text{O}_{28}(\text{SeO}_3)_3)_2(\text{M}(\text{H}_2\text{O})_4)]^{14-}$ ($\text{M}^{2+} = \text{Mn}^{2+}$, Co^{2+} , Zn^{2+}) (**2–4**) were isolated based on structurally relevant $\{\text{VO}_5\}$ -capped $\{\text{B-}\alpha\text{-SeV}_9\}$ clusters. Preliminary results indicated that **2–4** showed excellent catalytic activities toward selective oxidation reaction of sulfide to corresponding sulfoxide under the mild condition. Specifically, compound **4** as a representative can convert sulfides to corresponding sulfoxides efficiently and can be reused at least four times. The isolation of unique cluster $[\text{SeV}_{10}\text{O}_{28}(\text{SeO}_3)_3]^{8-}$ and the discovery of the *in-situ* formed building block $[\text{SeV}_{10}\text{O}_{28}(\text{SeO}_3)_3]^{8-}$ provide two new types of topology to the limited family of vanadium-based building blocks, and inspire chemists to investigating their pertinent synthetic and applied chemistry.

Experimental Section

Material and physical measurements

KVO_3 , SeO_2 , $\text{Zn}(\text{Ac})_2 \cdot 2\text{H}_2\text{O}$, $\text{Mn}(\text{Ac})_2 \cdot 4\text{H}_2\text{O}$, $\text{Co}(\text{Ac})_2 \cdot 4\text{H}_2\text{O}$ and other chemical reagents were acquired from commercial sources and used directly. IR spectra were conducted on a Bruker VERTEX 70 IR spectrometer (KBr pellets) recording in the range of 4000–450 cm^{-1} . Powder X-ray diffraction (XRD) patterns were obtained by employing a Bruker D8 ADVANCE diffractometer with $\text{Cu K}\alpha$ radiation (the value of λ is 1.54056 \AA). TG analyses were measured by a Perkin-Elmer TGA7 instrument under flowing N_2 (heating rate, 10 $^\circ\text{C min}^{-1}$). The quantitative analyses of Se, V, Mn, Co and Zn elements were achieved by PerkinElmer Optima 2100 DV inductively coupled plasma optical-emission spectrometer. Electron paramagnetic resonance (EPR) were all conducted on a Bruker EMX-10/12 spectrometer in the X-band at room temperature. X-ray photoelectron spectroscopy (XPS) were performed on an Axis Ultra x-ray photoelectron spectroscope equipped with monochromatic $\text{Al K}\alpha$ (1486.7 eV) radiation. Solution ^{51}V NMR spectrum was collected at the

FULL PAPER

Bruker AVANCE III HD 500 MHz (11.7 T) liquid instrument with a BBO 500 S2 probe, and the pulse program is onepulse. The chemical shift is using V_2O_5 as reference at -615 ppm.

Preparation of $K_6H_2[SeV_{10}O_{28}(SeO_3)_3] \cdot 14H_2O$ (1): Under stirring, solid SeO_2 (0.132 g, 1.2 mmol) was added in a 10 mL aqueous solution containing KVO_3 (0.414 g, 3 mmol). The pH value of the solution was maintained at about 3.3–3.6 with glacial acetic acid, and followed by addition of KCl solid (0.075 g, 1 mmol). The obtained red solution was heated to 90 °C for 0.5 h. After cooling down to room temperature, filtration and slow evaporation of the solution, dark red needle crystals were collected after 3–7 days. Yield: 0.153 g (29.9% based on V). In addition, a few orange crystals of decavanadate would be obtained from the remaining solution after several days. Elemental analysis calcd (%): Se, 16.52; V, 26.64. Found: Se, 16.67; V, 26.10. IR (KBr, cm^{-1}): 3432 (w), 1627 (m), 950 (s), 878 (s), 798 (sh), 738 (s), 621 (sh), 510 (m). TGA (weight loss): the first step 25–293 °C, 13.6%; the second step 293–500 °C, 23%. ^{51}V NMR (293 K, D_2O/H_2O) (chemical shifts, ppm): -614.7 , -696.5 , -714.6 , -738.4 .

Method 1 for syntheses of $K_6H_8[(SeV_{10}O_{28}(SeO_3)_3)_2(M(H_2O)_4)] \cdot 24H_2O$ (M = Mn^{2+} (2), Co^{2+} (3), Co^{2+} (4)): Under stirring, solid SeO_2 (0.132 g, 1.2 mmol) was added in a 10 mL aqueous solution containing KVO_3 (0.414 g, 3 mmol). A few minutes later, the pH value of the solution was first adjusted to 3.0–3.3 with glacial acetic acid. After the mixture being stirred for 10 minutes at room temperature, $Mn(Ac)_2 \cdot 4H_2O$ (0.049 g, 0.20 mmol) for 2 or $Co(Ac)_2 \cdot 4H_2O$ (0.050 g, 0.20 mmol) for 3 or $Zn(Ac)_2 \cdot 2H_2O$ (0.048 g, 0.20 mmol) for 4 was added, respectively, and the pH value of the solution was maintained at 3.3–3.6 with 3.0 mol L^{-1} KOH solution. The obtained red solution was heated to 90 °C for 0.5 h. After cooling down to room temperature, filtration and slow evaporation of the solution, dark red block crystals for 2–4 were collected after 3–7 days. Yield: 0.160 g (29.0% based on V) for 2, 0.153 g (28.0% based on V) for 3, and 0.274 g (49.6% based on V) for 4. Elemental analysis calcd (%) for 2: Se, 17.37; Mn, 1.51; V, 28.02; Found: Se, 17.84; Mn, 1.55; V, 27.83. Elemental analysis calcd (%) for 3: Se, 17.35; Co, 1.62; V, 27.99. Found: Se, 16.95; Co, 1.65; V, 27.35. Elemental analysis calcd (%) for 4: Se, 17.32; Zn, 1.79; V, 27.94. Found: Se, 17.77; Zn, 1.85; V, 28.52. IR (KBr, cm^{-1}): 3434 (w), 1624 (m), 955 (s), 860 (s), 803 (s), 753 (s), 557 (m) for 2; 3440 (w), 1625 (m), 955 (s), 862 (s), 801 (s), 752 (s), 556 (m) for 3; 3470 (w), 1625 (m), 956 (s), 867 (s), 803 (s), 753 (s), 558 (m) for 4. TGA (weight loss): the first step 25–293 °C, 11.8% for 2, 11.9% for 3, 12.0% for 4; the second step 293–1000 °C, 22.9% for 2, 23.5% for 3, 23.7% for 4. ^{51}V NMR (293 K, D_2O/H_2O) for dimagnetic 4 (chemical shifts, ppm): -615.3 , -698.1 , -716.6 , -734.4 .

Method 2 for syntheses of compounds 2–4: precursor 1 (0.19 g, 0.1 mmol) was completely dissolved in 10 mL distilled water at 90 °C. After 3 min stirring, $Mn(Ac)_2 \cdot 4H_2O$ (0.011 g, 0.05 mmol) for 2, or $Co(Ac)_2 \cdot 4H_2O$ (0.018 g, 0.05 mmol) for 3, or $Zn(Ac)_2 \cdot 2H_2O$ (0.018 g, 0.05 mmol) for 4 was added was added to the solution. The resulting solution was kept at 90 °C in a water bath for 0.5 h and then cooled to room temperature and filtered. Slow evaporation at room temperature resulted in dark red block crystals for 2–4 after about two weeks.

X-ray crystallography: The single crystals 1–4 were directly fixed on a loop and kept at 150.0 K during data collection on a Bruker D8 VENTURE PHOTON II CCD diffractometer with $Mo K\alpha$ radiation (the value of λ is 0.71073 Å). After the data reduction,²³ Olex2 was applied to analyse the structures, by which it was first solved with the ShelXT structure solution program by the utilization of direct methods and then refined with the ShelXL-2018/3 refinement package using least squares minimisation.²⁴ In addition, all the atoms are refined anisotropically in the final refinement cycle, only few harsh constraints have been used in order to eliminate the ADP alert of few atoms. And some lattice water molecules were located by Fourier map, whereas the rest lattice molecules were determined by TGA results. All H atoms on water molecules in the molecular formula were directly included. Crystallographic data of 1–4 have been deposited in the

Cambridge Crystallographic Data Center with CCDC numbers: 1923303–1923306. Crystal data and structure refinement parameters are detailed in Table S1.

General procedure for the selective oxidation of sulfides: The typical experimental procedure for the catalytic oxidation of various sulfides were carried out in a WP-TEC-102HC parallel from WATTCAS™ (Figure S10). Generally, 2 μ mol of catalyst, 1 mmol of sulfides, 3 mmol of TBHP and 2.5 mL methanol were charged in the reaction tube (50 mL) at the room temperature (25 °C) with constant stirring during the whole reactions. At regular intervals, an aliquot of sample solution was taken directly from the reaction mixture with a microsyringe and the liquid was analysed by gas chromatography (GC) using naphthalene as the internal standard. As for the recycling experiment, the POV catalyst was recovered by filtration at the end of each cycle, and then washed thoroughly (at least three times) by methanol, which was further dried at 60 °C in oven and reused for the successive run under the identical reaction conditions.

Acknowledgements

This work was supported by the National Natural Science Foundation of China (21573056).

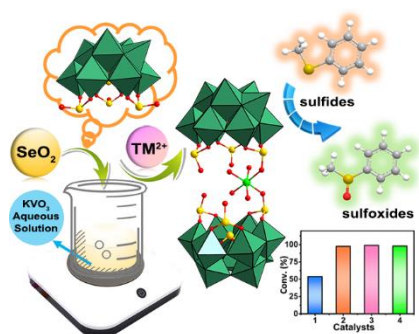
Keywords: Keggin • polyoxovanadate • vanadoselenite • heterogeneous catalysts • oxidation of sulfides

- [1] (a) H. N. Miras, J. Yan, D.-L. Long, L. Cronin, *Chem. Soc. Rev.* **2012**, *41*, 7403–7430; (b) Y.-F. Song, R. Tsunashima, *Chem. Soc. Rev.* **2012**, *41*, 7384–7402; (c) S.-S. Wang, G.-Y. Yang, *Chem. Rev.* **2015**, *115*, 4893–4962; (d) J. He, J. Li, Q. Han, C. Si, G. Niu, M. Li, J. Wang, J. Niu, *ACS Appl. Mater. Interfaces* **2020**, *12*, 2199–2206; (e) J. He, Q. Han, J. Li, Z. Shi, X. Shi, J. Niu, *J. Cat.* **2019**, *376*, 161–167; (f) J.-W. Zhao, Y.-Z. Li, L.-J. Chen, G.-Y. Yang, *Chem. Commun.* **2016**, *52*, 4418–4445; (g) P. Ma, F. Hu, H. Wu, X. Liu, J. Wang, J. Niu, *J. Lumin.* **2020**, *217*, 116760–116766; (h) H. Wu, B. Yan, R. Liang, V. Singh, P. Ma, J. Wang, J. Niu, *Dalton Trans.* **2020**, *49*, 388–394. (i) J. M. Cameron, D. J. Wales, G. N. Newton, *Dalton Trans.* **2018**, *47*, 5120–5136; (j) A. Bijelic, M. Aureliano and A. Rompel, *Chem. Commun.* **2018**, *54*, 1153–1169; (k) P. Ma, F. Hu, J. Wang, J. Niu, *Coord. Chem. Rev.* **2019**, *378*, 281–309; (l) D. Li, P. Ma, J. Niu and J. Wang, *Coord. Chem. Rev.*, **2019**, *392*, 49–80.
- [2] (a) J. Forster, B. Rösner, R. H. Fink, L. C. Nye, I. Ivanovic-Burmazovic, K. Kastner, J. Tucher, C. Streb, *Chem. Sci.* **2013**, *4*, 418–424; (b) J. Zhang, Y. Huang, G. Li, Y. Wei, *Coord. Chem. Rev.* **2019**, *378*, 395–414; (c) C. Zhang, M. Zhang, H. Shi, Q. Zeng, D. Zhang, Y. Zhao, Y. Wang, P. Ma, J. Wang, J. Niu, *Chem. Commun.* **2018**, *54*, 5458–5461; (d) S. Chen, Y. Liu, J. Guo, P. Li, Z. Huo, P. Ma, J. Niu, J. Wang, *Dalton Trans.* **2015**, *44*, 10152–10155; (e) R. Wan, P. Ma, M. Han, D. Zhang, C. Zhang, J. Niu, J. Wang, *Dalton Trans.* **2017**, *46*, 5398–5405.
- [3] (a) Y. Zhang, H. Gan, C. Qin, X. Wang, Z. Su, M. J. Zaworotko, *J. Am. Chem. Soc.* **2018**, *140*, 17365–17368; (b) K. Y. Monakhov, W. Bensch, P. Kögerler, *Chem. Soc. Rev.* **2015**, *44*, 8443–8483; (c) Y. Gao, Y. Chi, C. Hu, *Polyhedron* **2014**, *83*, 242–258.
- [4] (a) R. R. Langesley, D. M. Kaphan, C. L. Marshall, P. C. Stair, A. P. Sattelberger, M. Delferro, *Chem. Rev.* **2019**, *119*, 2128–2191; (b) K. Wang, Q. Xu, P. Ma, C. Zhang, J. Wang, J. Niu, *CrystEngComm* **2018**, *20*, 6273–6279; (c) J. Dong, J. Hu, Y. Chi, Z. Lin, B. Zou, S. Yang, C. L. Hill, C. Hu, *Angew. Chem. Int. Ed.* **2017**, *56*, 4473–4477; (d) G. Wang, P. Ma, D. Zhang, J. Niu, J. Wang, *J. Alloys Compd.* **2016**, *686*, 1032–1036; (e) M. G. Sorolla, X. Wang, T. Makarenko, A. J. Jacobson, *Chem. Commun.* **2019**, *55*, 342–344; (f) Y. Ji, J. Hu, J. Biskupek, U. Kaiser, Y.-F. Song, C. Streb, *Chem. - Eur. J.* **2017**, *23*, 16637–16643; (g) J.-J. Chen, M. D. Symes, S.-C. Fan, M.-S. Zheng, H. N. Miras, Q.-F. Dong, L. Cronin, *Adv. Mater.* **2015**, *27*, 4649–4654.
- [5] (a) Y. Hayashi, *Coord. Chem. Rev.* **2011**, *255*, 2270–2280; (b) K. Y. Monakhov, W. Bensch, P. Kögerler, *Chem. Soc. Rev.* **2015**, *44*, 8443–

FULL PAPER

- 8483; (c) J.-K. Li, C.-W. Hu, *Chin. J. Inorg. Chem.* **2015**, *31*, 1705–1725; (d) Y. Gao, X. Li, C. Hu, *Prog. Chem.* **2011**, *23*, 1050–1059.
- [6] (a) C. M. Flynn Jr., M. T. Pope, *Inorg. Chem.* **1970**, *9*, 2009–2014; (b) A. Kobayashi, Y. Sasaki, *Chem. Lett.* **1975**, *4*, 1123–1124; (c) D. Liu, Y. Lu, H.-Q. Tan, W.-L. Chen, Z.-M. Zhang, Y.-G. Li, E.-B. Wang, *Chem. Commun.* **2013**, *49*, 3673–3675; (d) W. Guo, J. Bacsa, J. van Leusen, K. P. Sullivan, H. Lv, P. Kögerler, C. L. Hill, *Inorg. Chem.* **2015**, *54*, 10604–10609.
- [7] (a) H. T. Evans Jr., J. A. Konner, *Am. Mineral.* **1978**, *63*, 863–868; (b) R. Kato, A. Kobayashi, Y. Sasaki, *J. Am. Chem. Soc.* **1980**, *102*, 6571–6572; (c) A. Müller, J. Döring, M. I. Khan, V. Wittneben, *Angew. Chem. Int. Ed. Engl.* **1991**, *30*, 210–212; (d) L.-H. Bi, U. Kortz, M. H. Dickman, S. Nellutla, N. S. Dalal, B. Keita, L. Nadjjo, M. Prinz, M. Neumann, *J. Cluster Sci.* **2006**, *17*, 143–165.
- [8] (a) A. Tripathi, T. Hughbanks, A. Clearfield, *J. Am. Chem. Soc.* **2003**, *125*, 10528–10529; (b) Y. Gao, Y. Xu, Y. Cao, C. Hu, *Dalton Trans.* **2012**, *41*, 567–571; (c) X. Wang, L. Liu, G. Zhang, A. J. Jacobson, *Chem. Commun.* **2001**, 2472–2473.
- [9] (a) D. Pitzschke, J. Wang, R.-D. Hoffmann, R. Pöttgen, W. Bensch, *Angew. Chem. Int. Ed.* **2006**, *45*, 1305–1308; (b) J. Zhou, J. Zhang, W.-H. Fang, G.-Y. Yang, *Chem. - Eur. J.* **2010**, *16*, 13253–13261.
- [10] (a) A. Müller, J. Döring, *Angew. Chem., Int. Ed. Engl.* **1988**, *27*, 1721; (b) G. Huan, M. A. Greaney, A. J. Jacobson, *J. Chem. Soc., Chem. Commun.* **1991**, 260–261; (c) S.-T. Zheng, J. Zhang, B. Li, G.-Y. Yang, *Dalton Trans.* **2008**, 5584–5587.
- [11] (a) X.-X. Hu, J.-Q. Xu, X.-B. Cui, J.-F. Song, T.-G. Wang, *Inorg. Chem. Commun.* **2004**, *7*, 264–267; (b) R. Kiebach, C. Näther, W. Bensch, *Solid State Sci.* **2006**, *8*, 964–970; (c) R. Kiebach, C. Näther, P. Kögerler, W. Bensch, *Dalton Trans.* **2007**, 3221–3223; (d) E. Antonova, B. Seidhofer, J. Wang, M. Hinz, W. Bensch, *Chem. - Eur. J.* **2012**, *18*, 15316–15322.
- [12] (a) J. Zhou, J.-W. Zhao, Q. Wei, J. Zhang, G.-Y. Yang, *J. Am. Chem. Soc.* **2014**, *136*, 5065–5071; (b) J. Ru, X. Ma, Y. Cui, M. Guo, J. Chen, X.-X. Li, *Cryst. Growth Des.* **2017**, *17*, 1384–1389; (c) X.-B. Cui, J.-Q. Xu, H. Meng, S.-T. Zheng, G.-Y. Yang, *Inorg. Chem.* **2004**, *43*, 8005–8009; (d) S.-T. Zheng, J. Zhang, G.-Y. Yang, *Inorg. Chem.* **2005**, *44*, 2426–2430.
- [13] H. Nakano, T. Ozeki, A. Yagasaki, *Inorg. Chem.* **2001**, *40*, 1816–1819.
- [14] (a) H. Li, H. Wu, R. Wan, Y. Wang, P. Ma, S. Li, J. Wang, J. Niu, *Dalton Trans.* **2019**, *48*, 2813–2821; (b) J. Jia, Y. Zhang, P. Zhang, P. Ma, D. Zhang, J. Wang, J. Niu, *RSC Adv.* **2016**, *6*, 108335–108342; (c) L. Yang, Y. Huo, J. Niu, *Dalton Trans.* **2013**, *42*, 364–367; (d) Z. Zhou, D. Zhang, L. Yang, P. Ma, Y. Si, U. Kortz, J. Niu, J. Wang, *Chem. Commun.* **2013**, *49*, 5189–5191; (e) J. W. Zhao, J. Zhang, S. T. Zheng, G. Y. Yang, *Chem. Commun.* **2008**, 570–572; (f) Z. Liu, W. Wang, J. Tang, W. Li, W. Yin, X. Fang, *Chem. Commun.* **2019**, 55, 6547–6550; (g) P. A. Abramov, E. V. Peresypkina, N. V. Izarova, C. Vicent, A. A. Zhdanov, N. B. Kompankov, T. Gutsule, M. N. Sokolov, *New J. Chem.* **2016**, *40*, 937–944.
- [15] R. Wan, H. Li, X. Ma, Z. Liu, V. Singh, P. Ma, C. Zhang, J. Niu, J. Wang, *Dalton Trans.* **2019**, *48*, 10327–10336.
- [16] (a) U. Kortz, M. G. Savelieff, B. S. Bassil, B. Keita, L. Nadjjo, *Inorg. Chem.* **2002**, *41*, 783–789; (b) A. C. Stowe, S. Nellutla, N. S. Dalal, U. Kortz, *Eur. J. Inorg. Chem.* **2004**, 3792–3797; (c) I. V. Kalinina, E. V. Peresypkina, N. V. Izarova, F. M. Nkala, U. Kortz, N. B. Kompankov, N. K. Moroz, M. N. Sokolov, *Inorg. Chem.* **2014**, *53*, 2076–2082; (d) J. M. Cameron, J. Gao, L. Vilà-Nadal, D.-L. Long, L. Cronin, *Chem. Commun.* **2014**, *50*, 2155–2157; (e) U. Kortz, M. G. Savelieff, F. Y. Abou Ghali, L. M. Khalil, S. A. Maalouf, D. I. Sinno, *Angew. Chem. Int. Ed.* **2002**, *41*, 4070–4073; (f) D. Yang, S. Li, P. Ma, J. Wang, J. Niu, *Inorg. Chem.* **2013**, *52*, 14034–14039; (g) J. Wang, P. Ma, Y. Wang, D. Zhang, J. Niu, J. Wang, *J. Phys. Chem. Solids* **2017**, *110*, 161–166.
- [17] (a) S. Wang, Y. Liu, Z. Zhang, X. Li, H. Tian, T. Yan, X. Zhang, S. Liu, X. Sun, L. Xu, F. Luo, S. Liu, *ACS Appl. Mater. Interfaces* **2019**, *11*, 12786–12796; (b) H. N. Miras, D. Stone, D.-L. Long, E. J. L. McInnes, P. Kögerler, L. Cronin, *Inorg. Chem.* **2011**, *50*, 8384–8391; (c) L. Chen, F. Jiang, Z. Lin, Y. Zhou, C. Yue, M. Hong, *J. Am. Chem. Soc.* **2005**, *127*, 8588–8589.
- [18] (a) C. Hureau, S. Blanchard, M. Nierlich, G. Blain, E. Rivière, J.-J. Girerd, E. Anxolabéhère-Mallart, G. Blondin, *Inorg. Chem.* **2004**, *43*, 4415–4426; (b) T. Hirotsu, A. Sonoda, H. Kanoh, K. Ooi, M. Seno, *J. Phys. Chem. B* **1997**, *101*, 4498–4507; (c) J.-P. Wang, P.-T. Ma, J. Li, H.-Y. Niu, J.-Y. Niu, *Chem. Asian J.* **2008**, *3*, 822–833.
- [19] (a) U. Lee, H.-C. Joo, K.-M. Park, S. S. Mal, U. Kortz, B. Keita, L. Nadjjo, *Angew. Chem. Int. Ed.* **2008**, *47*, 793–796; (b) J.-H. Son, C. A. Ohlin, E. C. Larson, P. Yu, W. H. Casey, *Eur. J. Inorg. Chem.* **2013**, 1748–1753.
- [20] (a) J. Liu, X. Wang, J. Ma, L. Meng, *Acta Chim. Sinica* **1999**, *57*, 769–774; (b) A. A. Shubin, D. F. Khabibulin, O. B. Lapina, *Catal. Today* **2009**, *142*, 220–226.
- [21] (a) M. Han, Y. Niu, R. Wan, Q. Xu, J. Lu, P. Ma, C. Zhang, J. Niu, J. Wang, *Chem. - Eur. J.* **2018**, *24*, 11059–11066; (b) J. Lu, X. Ma, V. Singh, Y. Zhang, P. Ma, C. Zhang, J. Niu, J. Wang, *Dalton Trans.* **2018**, *47*, 5279–5285; (c) J. Lu, Y. Wang, X. Ma, Y. Niu, V. Singh, P. Ma, C. Zhang, J. Niu, J. Wang, *Dalton Trans.* **2018**, *47*, 8070–8077; (d) B.-B. Lu, J. Yang, Y.-Y. Liu, J.-F. Ma, *Inorg. Chem.* **2017**, *56*, 11710–11720.
- [22] (a) J.-K. Li, X.-Q. Huang, S. Yang, H.-W. Ma, Y.-N. Chi, C.-W. Hu, *Inorg. Chem.* **2015**, *54*, 1454–1461; (b) K. Wang, Q. Xu, P. Ma, C. Zhang, J. Wang, J. Niu, *CrystEngComm* **2018**, *20*, 6273–6279; (c) J.-K. Li, J. Dong, C.-P. Wei, S. Yang, Y.-N. Chi, Y.-Q. Xu, C.-W. Hu, *Inorg. Chem.*, **2017**, *56*, 5748–5756; (d) K. Wang, Y. Niu, D. Zhao, Y. Zhao, P. Ma, D. Zhang, J. Wang, J. Niu, *Inorg. Chem.* **2017**, *56*, 14053–14059; (e) J. Li, X. Huang, S. Yang, Y. Xu, C. Hu, *Cryst. Growth Des.* **2015**, *15*, 1907–1914.
- [23] SAINT, *Program for Data Extraction and Reduction*, Bruker AXS, Inc., Madison, WI, **2001**.
- [24] (a) O. V. Dolomanov, L. J. Bourhis, R. J. Gildea, J. A. K. Howard, H. Puschmann, *J. Appl. Cryst.* **2009**, *42*, 339–341; (b) G. M. Sheldrick, *Acta Crystallogr., Sect. A: Found. Crystallogr.* **2008**, *64*, 112–122; (c) G. M. Sheldrick, *Acta Cryst.* **2015**, *A71*, 3–8; (d) G. M. Sheldrick, *SHELXL-2018/3, Program for Crystal Structure Refinement*, University of Göttingen, Germany, **2018**.

Entry for the Table of Contents



New topology of polyoxovanadates: A rare example of lacunary Keggin-type vanadoselenite $[\text{SeV}_{10}\text{O}_{28}(\text{SeO}_3)_3]^{8-}$ ($\{\text{Se}_4\text{V}_{10}\}$) was readily obtained, which shows sufficient reactivity with divalent transition metals (TMs) to form a new series of TM-sandwiched complexes $\{(\text{Se}_4\text{V}_{10})_2\text{M}\}$ ($\text{M} = \text{Mn}, \text{Co}, \text{Zn}$). Such new TM-derivatives can efficiently catalyze heterogeneous oxidation of sulfides in high conversion and selectivity under mild conditions.